Analytic, group-theoretic density profiles for confined, correlated *N*-body systems

W. B. Laing,* M. Dunn, and D. K. Watson
University of Oklahoma, Homer L. Dodge Department of Physics and Astronomy, Norman, Oklahoma 73019, USA
(Received 18 July 2006; published 5 December 2006)

Confined quantum systems involving *N* identical interacting particles are to be found in many areas of physics, including condensed-matter, atomic, and chemical physics. A beyond-mean-field perturbation method that is applicable, in principle, to weakly, intermediate, and strongly interacting systems has been set forth by the authors in a previous series of papers. Dimensional perturbation theory was used, and in conjunction with group theory, an analytic beyond-mean-field correlated wave function at lowest order for a system under spherical confinement with a general two-body interaction was derived. In the present paper, we use this analytic wave function to derive the corresponding lowest-order, analytic density profile and apply it to the example of a Bose-Einstein condensate.

DOI: 10.1103/PhysRevA.74.063605 PACS number(s): 03.75.Hh, 31.15.Hz, 03.65.Ge, 31.15.Md

I. INTRODUCTION

Confined quantum systems are widespread across many areas of physics. They include, among other examples, quantum dots [1], two-dimensional electronic systems in a corbino disk geometry [2], Bose-Einstein condensates (BECs) [3], rotating superfluid helium systems [4], and atoms (where the massive nucleus provides the confining potential for the electrons). These new (and sometimes old) systems possess from a few tens to millions of particles and present a challenge for existing *N*-body methods when the mean-field approach fails [5].

These systems span an enormous range in interparticle interaction strength. For example, a gaseous BEC is typically a weakly interacting system for which a mean-field description is perfectly adequate. On the other hand, a superfluid helium system is a strongly interacting system. In this regard we note that the scattering length of a gaseous BEC tuned by a magnetic field can cover the entire range of interactions, from weakly interacting to strongly interacting. A few of the methods that have been applied to strongly interacting systems include the coupled cluster method (CCM) [6], the method of correlated basis functions (CBFs) [7], density-functional theory [8], and quantum Monte Carlo methods [5,9,10].

Dimensional perturbation theory (DPT) [11,12] provides a systematic approach to the study of correlation in quantum confined systems. This method takes advantage of the high degree of symmetry possible among identical particles in higher dimensions to obtain an analytic description of the confined quantum system—without making any assumptions about the number of particles or the strength of interparticle interactions. Because the perturbation parameter is the inverse of the dimensionality of space ($\delta=1/D$), DPT is equally applicable to weakly or strongly interacting systems. Another important advantage of DPT is that low-order DPT calculations are essentially *analytic* in nature [13]. As a consequence the number of atoms enters into the calculations as a parameter, and so, in principle, results for any *N* are obtainable from a single calculation [14]. Also, even the lowest-order result includes correlation, and so DPT may also be used to explore the transition between weakly interacting systems and those which are strongly interacting. These results can be systematically improved by going to higher order [15].

In principle, excited states at low order in DPT are obtained from the same analytic calculation [14]. They only differ in the number of quanta in the different normal modes. Higher orders in the DPT expansion of excited states can also be calculated [15].

In past papers we have begun to apply dimensional perturbation theory to calculate the first-order ground-state energy and normal-mode frequencies of spherically confined quantum systems [13,14,16–18]. In our last paper, we developed the formalism for deriving the lowest-order DPT wave function for an $L=0$ spherically confined quantum system (see Ref. [18] here also referred to as Paper I). In the present paper, we use the formalism developed in Paper I to calculate the lowest-order DPT density profile of the spherically confined quantum system. We apply these results to the specific case of a BEC for which the density profile is a directly observable manifestation of the quantized behavior of the confined quantum system.

Section II provides a brief overview of the tools used. Section III discusses the $L=0$, D-dimensional, N-body Schrödinger equation where L is the total angular momentum of the system. Sections IV–VII provide a summary of the relevant results from our previous work, particularly from Paper I. Then in Sec. VIII the lowest-order density profile is derived from the lowest-order wave function of Paper I (summarized Secs. IV–VII), while Sec. IX discusses how it is possible to optimize our lowest-order result by minimizing the contribution from higher-order terms. Sections X and XI apply these results to the case of a BEC. Section X sets up the problem for a BEC, assuming a hard-sphere interatomic potential at $D=3$, while Sec. XI discusses the details of minimizing the contribution from higher-order terms. Section XII discusses the results for a BEC. Section XIII presents our conclusions.

*Electronic address: Laing@ou.edu

II. TOOLBOX

The tools used to describe large-N correlated wave functions are carefully chosen to maximize the use of symmetry and minimize the dependence on numerical computation. We handle the massive number of interactions for large N ($\sim N^2/2$ two-body interactions) by bringing together three theoretical methods.

The first, DPT [11,12], is chosen because its $D\to\infty$ equation yields a maximally symmetric configuration for N identical particles which allows an analytic solution. Higher orders yield insight into fundamental motions as well as a framework for successive approximations. The second method is the *FG* method of Wilson, Decius, and Cross [19]. This seminal method has long been used in quantum chemistry to study vibrations of polyatomic molecules. It directly relates the structure of the Schrödinger equation to the coordinate set which describes the normal modes of the system. The third method, the use of group theoretic techniques [19,20], takes full advantage of the point-group symmetry in the $D\to\infty$ limit.

III. D-DIMENSIONAL N-BODY SCHRÖDINGER EQUATION

The Schrödinger equation for an N-body system of particles confined by a spherically symmetric potential with a two-body potential g_{ij} is

$$H\Psi = \left[\sum_{i=1}^{N} h_i + \sum_{i=1}^{N-1}\sum_{j=i+1}^{N} g_{ij}\right]\Psi = E\Psi. \tag{1}$$

In a D-dimensional Cartesian space

$$h_i = -\frac{\hbar^2}{2m_i}\sum_{\nu=1}^{D}\frac{\partial^2}{\partial x_{i\nu}^2} + V_{\rm conf}\left(\sqrt{\sum_{\nu=1}^{D} x_{i\nu}^2}\right), \tag{2}$$

and

$$g_{ij} = V_{\rm int}\left(\sqrt{\sum_{\nu=1}^{D}(x_{i\nu}-x_{j\nu})^2}\right) \tag{3}$$

are the single-particle Hamiltonian and the two-body interaction potential, respectively, $x_{i\nu}$ is the νth Cartesian component of the ith particle, and $V_{\rm conf}$ is the confining potential.

A. Effective S-wave Schrödinger equation

It is desirable to transform from Cartesian to internal coordinates. A convenient internal coordinate system for confined spherically symmetric ($L=0$) systems is

$$r_i = \sqrt{\sum_{\nu=1}^{D} x_{i\nu}^2} \quad (1\leqslant i\leqslant N),$$

and

$$\gamma_{ij} = \cos(\theta_{ij}) = \left(\sum_{\nu=1}^{D} x_{i\nu}x_{j\nu}\right)/r_i r_j \tag{4}$$

$(1\leqslant i<j\leqslant N)$, which are the D-dimensional scalar radii r_i of the N particles from the center of the confining potential and the cosines γ_{ij} of the $N(N-1)/2$ angles between the radial vectors. Under this coordinate change the effective S-wave Schrödinger equation in these internal coordinates becomes

$$\left\{\sum_i\left[-\frac{\hbar^2}{2m_i}\left(\frac{\partial^2}{\partial r_i^2}+\frac{D-1}{r_i}\frac{\partial}{\partial r_i}+\sum_{j\neq i}\sum_{k\neq i}\frac{\gamma_{jk}-\gamma_{ij}\gamma_{ik}}{r_i^2}\frac{\partial^2}{\partial\gamma_{ij}\partial\gamma_{ik}}\right.\right.$$
$$\left.\left.-\frac{D-1}{r_i^2}\sum_{j\neq i}\gamma_{ij}\frac{\partial}{\partial\gamma_{ij}}\right)+V_{\rm conf}(r_i)\right]+\sum_{i=1}^{N-1}\sum_{j=i+1}^{N}V_{\rm int}(r_{ij})\Bigg\}\Psi$$
$$= E\Psi, \tag{5}$$

where $(r_{ij})^2=(r_i)^2+(r_j)^2-2r_ir_j\gamma_{ij}$.

B. Jacobian-weighted Schrödinger equation

Dimensional perturbation theory utilizes a similarity transformation so that the kinetic-energy operator is transformed into a sum of two types of terms, namely, derivative terms *and* a repulsive centrifugal-like term. The latter repulsive centrifugal-like term stabilizes the system against collapse in the large-D limit when attractive interparticle potentials are present. Low orders of the dimensional $(1/D)$ expansion of the similarity-transformed Schrödinger equation are then exactly soluble for any value of N. In the $D\to\infty$ limit the derivative terms drop out resulting in a static problem, while large-D corrections correspond to simple harmonic normal-mode oscillations about the infinite-dimensional structure. (See Secs. IV–VII below.)

In Paper I the weight function was chosen to be the square root of the inverse of the Jacobian J, where [21] $J=(r_1r_2\cdots r_N)^{D-1}\Gamma^{(D-N-1)/2}$ and Γ is the Gramian determinant, the determinant of the matrix whose elements are γ_{ij} (see Appendix D of Ref. [13]), so that the similarity-transformed wave function Φ and operators $\tilde{O}$ are $\Phi=J^{1/2}\Psi$ and $\tilde{O}=J^{1/2}\hat{O}J^{-1/2}$, respectively. Under this Jacobian transformation, a first derivative of an internal coordinate is the conjugate momentum to that coordinate. The matrix elements of coordinates and their derivatives between the lowest-order normal-mode functions, which are involved in the development of higher-order DPT expansions, are much easier to calculate since the weight function in the integrals is now unity.

Carrying out the above Jacobian transformation of the Schrödinger equation of Eq. (1), we obtain [21]

$$(T+V)\Phi = E\Phi, \tag{6}$$

where

$$T=\hbar^2\sum_{i=1}^{N}\left(-\frac{1}{2m_i}\frac{\partial^2}{\partial r_i^2}-\frac{1}{2m_ir_i^2}\sum_{j\neq i}\sum_{k\neq i}\frac{\partial}{\partial\gamma_{ij}}(\gamma_{jk}-\gamma_{ij}\gamma_{ik})\frac{\partial}{\partial\gamma_{ik}}\right.$$
$$\left.+\frac{N(N-2)+(D-N-1)^2(\Gamma^{(i)}/\Gamma)}{8m_ir_i^2}\right) \tag{7}$$

and

$$V = \sum_{i=1}^{N} V_{\text{conf}}(r_i) + \sum_{i=1}^{N-1} \sum_{j=i+1}^{N} V_{\text{int}}(r_{ij}). \tag{8}$$

Equation (7) for T is explicitly self-adjoint since the weight function W for the matrix elements is equal to unity. The similarity-transformed Hamiltonian for the energy eigenstate Φ is $H=(T+V)$.

IV. INFINITE-D ANALYSIS: LEADING-ORDER ENERGY

Following Paper I, we begin the perturbation analysis by defining dimensionally scaled variables:

$$\bar{r}_i = r_i/\kappa(D), \quad \bar{E} = \kappa(D)E, \quad \text{and} \quad \bar{H} = \kappa(D)H, \tag{9}$$

where $\kappa(D)$ is a dimension-dependent scale factor, which regularizes the large-dimension limit. From Eq. (7) the kinetic energy T scales in the same way as $1/r^2$, so the scaled version of Eq. (6) becomes

$$\bar{H}\Phi = \left(\frac{1}{\kappa(D)}\bar{T} + \bar{V}_{\text{eff}}\right)\Phi = \bar{E}\Phi, \tag{10}$$

where barred quantities indicate that the variables are now in scaled units. The centrifugal-like term in T of Eq. (7) has quadratic D dependence so the scale factor $\kappa(D)$ must also be quadratic in D, otherwise the $D\to\infty$ limit of the Hamiltonian would not be finite. The precise form of $\kappa(D)$ depends on the particular system and is chosen so that the result of the scaling is as simple as possible. In previous work [13] we have chosen $\kappa(D)=(D-1)(D-2N-1)/(4Z)$ for the S-wave, N-electron atom; Ωl_{ho} for the N-electron quantum dot where $\Omega=(D-1)(D-2N-1)/4$, and the dimensionally scaled harmonic oscillator length and trap frequency, respectively, are $l_{\text{ho}}=\sqrt{\frac{\hbar}{m^*\bar{\omega}_{\text{ho}}}}$ and $\bar{\omega}_{\text{ho}}^2=\Omega^3\omega_{\text{ho}}^2$; and $D^2\bar{a}_{\text{ho}}$ for the BEC where $\bar{a}_{\text{ho}}=\sqrt{\frac{\hbar}{m\bar{\omega}_{\text{ho}}}}$ and $\bar{\omega}_{\text{ho}}=D^3\omega_{\text{ho}}$. In the $\delta\to 0$ $(D\to\infty)$ limit, where

$$\delta \equiv 1/D, \tag{11}$$

the factor of $\kappa(D)$ in the denominator of Eq. (10) suppresses the derivative terms leaving behind a centrifugal-like term in an effective potential,

$$\bar{V}_{\text{eff}}(\bar{r},\gamma;\delta=0) = \sum_{i=1}^{N}\left(\frac{\hbar^2}{8m_i\bar{r}_i^2}\frac{\Gamma^{(i)}}{\Gamma} + \bar{V}_{\text{conf}}(\bar{r},\gamma;\delta=0)\right) + \sum_{i=1}^{N-1}\sum_{j=i+1}^{N}\bar{V}_{\text{int}}(\bar{r},\gamma;\delta=0), \tag{12}$$

in which the particles become frozen. In the $D\to\infty$ $(\delta\to 0)$ limit, the excited states collapse onto the ground state at the minimum of V_{eff}.

We assume a totally symmetric, large-dimension configuration at which the effective potential is a minimum. The N particles are arranged on a hypersphere, each particle with a radius $\bar{r}_\infty$ from the center of the confining potential. Furthermore, the angle cosines between each pair of particles take on the same value, $\bar{\gamma}_\infty$, i.e.,

$$\lim_{D\to\infty} \bar{r}_i = \bar{r}_\infty \quad (1 \leqslant i \leqslant N),$$

$$\lim_{D\to\infty} \gamma_{ij} = \bar{\gamma}_\infty \quad (1 \leqslant i < j \leqslant N). \tag{13}$$

This configuration for $N=1$, 2, 3, and 4 is comparable to the sequence of arrangements of hydrogen atoms in LiH, H_2O, NH_3, and CH_4. In this analogy, the heterogeneous atom represents the center of the confining potential [22]. (This symmetric high-dimensional structure is also not unlike the localized structure found in a hyperspherical treatment of the confined two-component normal Fermi gas in the $N\to\infty$ limit [23].)

In scaled units the $D\to\infty$ approximation for the energy is simply the effective potential minimum, i.e.,

$$\bar{E}_\infty = \bar{V}_{\text{eff}}(\bar{r}_\infty, \bar{\gamma}_\infty; \delta=0). \tag{14}$$

In this $D\to\infty$ approximation, the centrifugal-like term that appears in $\bar{V}_{\text{eff}}$, which is nonzero even for the ground state, is a zero-point energy contribution satisfying the minimum uncertainty principle [24].

Beyond-mean-field effects are already present in this approximation. This may be seen in the value of $\bar{\gamma}_\infty$, the $D\to\infty$ expectation value for the interparticle angle cosine [see Eqs. (13) and (17)]. In the mean-field approximation the expectation value for the interparticle angle cosine for the $L=0$ states considered in this paper is zero. The fact that $\bar{\gamma}_\infty$ is *not* zero is an indication that beyond-mean-field effects are included even in the $D\to\infty$ limit.

This symmetric structure in which all N particles are equidistant and equiangular from every other particle can only exist in a higher-dimensional space and is impossible in a three-dimensional space unless $N\leqslant 4$ (see above). That this high dimensional structure makes sense can be seen as follows. As we have noted above, $\bar{r}_\infty$ and $\bar{\gamma}_\infty$ are the lowest-order DPT expectation values for $\bar{r}_i$ and γ_{ij}. This would indicate that the expectation values for the radii and interparticle angles for actual $D=3$ systems should have values corresponding to structures that can only exist in higher $(D>3)$ dimensional spaces. Accurate configuration interaction calculations for atoms in three dimensions do indeed have expectation values for the radii and interelectron angles which define higher dimension structures [25].

This highly symmetric, $D\to\infty$ structure imparts a point-group structure to the system which is isomorphic to the symmetric group of N identical objects [20], S_N, and allows for a largely analytic solution to the problem, even though the number of degrees of freedom becomes very large when N is large. The $D\to\infty$ approximation may also be systematically improved by using it as the starting point for a perturbation expansion (DPT) [15]. In this regard, the S_N symmetry greatly simplifies this task since the interaction terms individually have to transform as a scalar under the S_N point group.

V. NORMAL-MODE ANALYSIS AND THE $1/D$ NEXT-ORDER ENERGY CORRECTION

In the $D\to\infty$ limit, the particles are frozen in a completely symmetric configuration (which is somewhat analogous to the Lewis structure in chemical terminology [26]). This configuration determines the $D\to\infty$ energy $\bar{E}_\infty$ but it is not a wave function as no nodal information is present. The large-dimension limit is a singular limit of the theory, so to obtain the lowest-order wave function we have to consider the next order in the perturbation expansion, which yields not only the $(1/D)^0$, i.e., leading-order wave function, but the order $(1/D)^1$ correction to the energy. The perturbation series has the form

$$\bar{E} = \bar{E}_\infty + \delta\sum_{j=0}^{\infty} (\delta^{1/2})^j \bar{E}_j,$$

$$\Phi(\bar{r}_i, \gamma_{ij}) = \sum_{j=0}^{\infty} (\delta^{1/2})^j \Phi_j. \tag{15}$$

In practice $\bar{E}_j=0\ \forall j$ odd. This next-order $1/D$ correction in the energy, but lowest-order in the wave function, can be viewed as involving small oscillations about the $D\to\infty$ structure (somewhat analogous to Langmuir oscillations [27]). As we shall see below, these are obtained from a harmonic equation, and so we refer to them as the energy and wave function at harmonic order.

To obtain this harmonic correction to the energy for large but finite values of D, we expand about the minimum of the $D\to\infty$ effective potential. We first define a position vector $\bar{\mathbf{y}}$, consisting of all $N(N+1)/2$ internal coordinates:

$$\bar{\mathbf{y}} = \begin{pmatrix} \bar{\mathbf{r}} \\ \boldsymbol{\gamma} \end{pmatrix} \quad \text{where } \boldsymbol{\gamma} = \begin{pmatrix} \gamma_{12} \\ \gamma_{13} \\ \underline{\gamma_{23}} \\ \gamma_{14} \\ \gamma_{24} \\ \underline{\gamma_{34}} \\ \gamma_{15} \\ \gamma_{25} \\ \vdots \\ \gamma_{N-2,N} \\ \gamma_{N-1,N} \end{pmatrix}, \quad \text{and } \bar{\mathbf{r}} = \begin{pmatrix} \bar{r}_1 \\ \bar{r}_2 \\ \vdots \\ \bar{r}_N \end{pmatrix}. \tag{16}$$

We then make the following substitutions for all radii and angle cosines:

$$\bar{r}_i = \bar{r}_\infty + \delta^{1/2}\bar{r}_i' \quad \text{and} \quad \gamma_{ij} = \bar{\gamma}_\infty + \delta^{1/2}\bar{\gamma}_{ij}'. \tag{17}$$

In all practical situations $\bar{V}_{\text{eff}}(\bar{\mathbf{y}};\delta)$ is a function of $\bar{\mathbf{y}}$ and δ, so we may obtain a power series in $\delta^{1/2}$ of the effective potential about the $D\to\infty$ symmetric minimum.

Defining a displacement vector of the internal displacement coordinates [primed in Eqs. (17)]

$$\bar{\mathbf{y}}' = \begin{pmatrix} \bar{\mathbf{r}}' \\ \bar{\boldsymbol{\gamma}}' \end{pmatrix} \quad \text{where } \bar{\boldsymbol{\gamma}}' = \begin{pmatrix} \bar{\gamma}_{12}' \\ \bar{\gamma}_{13}' \\ \underline{\bar{\gamma}_{23}'} \\ \bar{\gamma}_{14}' \\ \bar{\gamma}_{24}' \\ \underline{\bar{\gamma}_{34}'} \\ \bar{\gamma}_{15}' \\ \bar{\gamma}_{25}' \\ \vdots \\ \bar{\gamma}_{N-2,N}' \\ \bar{\gamma}_{N-1,N}' \end{pmatrix}, \quad \text{and } \bar{\mathbf{r}}' = \begin{pmatrix} \bar{r}_1' \\ \bar{r}_2' \\ \vdots \\ \bar{r}_N' \end{pmatrix}, \tag{18}$$

we find

$$\bar{V}_{\text{eff}}(\bar{\mathbf{y}}';\delta) = [\bar{V}_{\text{eff}}]_{\delta^{1/2}=0} + \frac{1}{2}\delta\left\{\sum_{\mu=1}^{P}\sum_{\nu=1}^{P}\bar{y}_\mu'\left[\frac{\partial^2\bar{V}_{\text{eff}}}{\partial\bar{y}_\mu\partial\bar{y}_\nu}\right]_{\delta^{1/2}=0}\bar{y}_\nu' + v_o\right\} + O(\delta^{3/2}), \tag{19}$$

where $P\equiv N(N+1)/2$ is the number of internal coordinates. The quantity v_o is just a constant term, independent of $\bar{y}_\mu'$, while the first term of the $O((\delta^{1/2})^2)$ term defines the elements of the Hessian matrix [28] $\boldsymbol{F}$ of Eq. (21) below. The derivative terms in the kinetic energy are taken into account by a similar series expansion, beginning with a harmonic-order term that is bilinear in $\partial/\partial\bar{\mathbf{y}}'$, i.e.,

$$\mathcal{T} = -\frac{1}{2}\delta\sum_{\mu=1}^{P}\sum_{\nu=1}^{P} G_{\mu\nu}\partial_{\bar{y}_\mu'}\partial_{\bar{y}_\nu'} + O(\delta^{3/2}), \tag{20}$$

where $\mathcal{T}$ is the derivative portion of the kinetic energy T [see Eq. (7)]. It follows from Eqs. (19) and (20) that $\boldsymbol{G}$ and $\boldsymbol{F}$, both constant matrices, are defined in the harmonic-order Hamiltonian as follows:

$$\hat{H}_0 = -\frac{1}{2}\partial_{\bar{\mathbf{y}}'}{}^T\boldsymbol{G}\partial_{\bar{\mathbf{y}}'} + \frac{1}{2}\bar{\mathbf{y}}'{}^T F\bar{\mathbf{y}}' + v_o. \tag{21}$$

Thus obtaining the harmonic-order wave function, and energy correction is reduced to solving a harmonic equation by finding the normal modes of the system.

FG matrix method for the normal modes and frequencies

We use the *FG* matrix method [19] to obtain the normal-mode vibrations and, thereby, the harmonic-order energy correction. A review of the *FG* matrix method is presented in Appendix A of Paper I, but the main results may be stated as follows. The bth normal-mode coordinate may be written as [Eq. (A9) of Paper I]

$$[\boldsymbol{q}']_b = \boldsymbol{b}^T\bar{\mathbf{y}}', \tag{22}$$

where the coefficient vector $\boldsymbol{b}$ satisfies the eigenvalue equation [Eq. (A10) of Paper I]

$$\boldsymbol{FGb} = \lambda_b \boldsymbol{b} \tag{23}$$

with the resultant secular equation [Eq. (A11) of Paper I] $\det(\boldsymbol{FG}-\lambda \boldsymbol{I})=0$. The coefficient vector also satisfies the normalization condition [Eq. (A12) of Paper I] $\boldsymbol{b}^T\boldsymbol{Gb}=1$. As can be seen from Eq. (A3) of Paper I the frequencies are given by $\lambda_b=\bar{\omega}_b^2$.

In an earlier paper [13] we solve these equations for the frequencies. The number of roots λ of the secular equation—there are $P\equiv N(N+1)/2$ roots—is potentially huge. However, due to the S_N symmetry of the problem discussed in Secs. V and VI of Paper I, there is a very significant simplification. The secular equation has only five distinct roots λ_μ, where μ is a label which runs over $\mathbf{0}^-$, $\mathbf{0}^+$, $\mathbf{1}^-$, $\mathbf{1}^+$, and $\mathbf{2}$, regardless of the number of particles in the system (see Refs. [13] and Sec. VI B). Thus the energy through harmonic order [see Eq. (25)] can be written in terms of the five distinct normal-mode vibrational frequencies which are related to the roots λ_μ of FG by

$$\lambda_\mu = \bar{\omega}_\mu^2. \tag{24}$$

The energy through harmonic order in δ is then [13]

$$\bar{E} = \bar{E}_\infty + \delta\left[\sum_{\mu=\{\mathbf{0}^\pm,\mathbf{1}^\pm,\mathbf{2}\}} \sum_{\mathsf{n}_\mu=0}^{\infty} \left(\mathsf{n}_\mu + \frac{1}{2}\right) d_{\mu,\mathsf{n}_\mu} \bar{\omega}_\mu + v_o\right], \tag{25}$$

where the n_μ are the vibrational quantum numbers of the normal modes of the same frequency $\bar{\omega}_\mu$ (n_μ counts the number of nodes in a given normal mode). The quantity d_{μ,n_μ} is the occupancy of the manifold of normal modes with vibrational quantum number n_μ and normal-mode frequency $\bar{\omega}_\mu$, i.e., it is the number of normal modes with the same frequency $\bar{\omega}_\mu$ and the same number of quanta n_μ. The total occupancy of the normal modes with frequency $\bar{\omega}_\mu$ is equal to the multiplicity of the root λ_μ, i.e., $d_\mu=\Sigma_{\mathsf{n}_\mu=0}^{\infty} d_{\mu,\mathsf{n}_\mu}$, where d_μ is the multiplicity of the μth root. The multiplicities of the five roots are [13]

$$d_{\mathbf{0}^+}=1, \quad d_{\mathbf{0}^-}=1, \quad d_{\mathbf{1}^+}=N-1,$$

$$d_{\mathbf{1}^-}=N-1, \quad d_{\mathbf{2}}=N(N-3)/2. \tag{26}$$

An analysis of the character of the normal modes reveals that the $\mathbf{2}$ normal modes are phonon, i.e., compressional, modes; the $\mathbf{1}^\pm$ modes show single-particle character, and the $\mathbf{0}^\pm$ normal modes in a harmonic confining potential describe center-of-mass and breathing motions [29].

VI. SYMMETRY OF THE F AND G MATRICES AND THE JACOBIAN-WEIGHTED WAVE FUNCTION

A. Q matrices in terms of simple invariant submatrices

Such a high degree of degeneracy of the frequencies in large-D, N-body quantum confinement problems indicates a very high degree of symmetry. The $\boldsymbol{F}$, $\boldsymbol{G}$, and $\boldsymbol{FG}$ matrices, which we generically denote by $\boldsymbol{Q}$, are $P\times P$ matrices. The S_N symmetry of the $\boldsymbol{Q}$ matrices ($\boldsymbol{F}$, $\boldsymbol{G}$, and $\boldsymbol{FG}$) allows us to write these matrices in terms of six simple submatrices which are invariant under S_N. We first define the number of γ_{ij} coordinates to be $M\equiv N(N-1)/2$, and let $\boldsymbol{I}_N$ be an $N\times N$ identity matrix, $\boldsymbol{I}_M$ an $M\times M$ identity matrix, $\boldsymbol{J}_N$ an $N\times N$ matrix of ones and $\boldsymbol{J}_M$ an $M\times M$ matrix of ones. Further, we let $\boldsymbol{R}$ be an $N\times M$ matrix such that $R_{i,jk}=\delta_{ij}+\delta_{ik}$, $\boldsymbol{J}_{NM}$ be an $N\times M$ matrix of ones, and $\boldsymbol{J}_{NM}^T=\boldsymbol{J}_{MN}$. These matrices are invariant under interchange of the particles, effected by the point group S_N. They also have a specific interpretation in the context of spectral graph theory (see Appendix B of Ref. [13]).

We can then write the $\boldsymbol{Q}$ matrices as

$$\boldsymbol{Q} = \begin{pmatrix} \boldsymbol{Q}_{\bar{r}'\bar{r}'} & \boldsymbol{Q}_{\bar{r}'\bar{\gamma}'} \\ \boldsymbol{Q}_{\bar{\gamma}'\bar{r}'} & \boldsymbol{Q}_{\bar{\gamma}'\bar{\gamma}'} \end{pmatrix} = \left(\begin{array}{c|c} Q_{i,j} & Q_{i,jk} \\ \hline Q_{ij,k} & Q_{ij,kl} \end{array}\right), \tag{27}$$

where the block $\boldsymbol{Q}_{\bar{r}'\bar{r}'}$ has dimension $(N\times N)$, block $\boldsymbol{Q}_{\bar{r}'\bar{\gamma}'}$ has dimension $(N\times M)$, block $\boldsymbol{Q}_{\bar{\gamma}'\bar{r}'}$ has dimension $(M\times N)$, and block $\boldsymbol{Q}_{\bar{\gamma}'\bar{\gamma}'}$ has dimension $(M\times M)$. As shown in Appendix B of Ref. [13],

$$\boldsymbol{Q}_{\bar{r}'\bar{r}'} = (Q_a - Q_b)\boldsymbol{I}_N + Q_b \boldsymbol{J}_N, \tag{28}$$

$$\left.\begin{aligned} \boldsymbol{Q}_{\bar{r}'\bar{\gamma}'} &= (Q_e - Q_f)\boldsymbol{R} + Q_f \boldsymbol{J}_{NM} \\ \boldsymbol{Q}_{\bar{\gamma}'\bar{r}'} &= (Q_c - Q_d)\boldsymbol{R}^T + Q_d \boldsymbol{J}_{NM}^T \end{aligned}\right\}, \tag{29}$$

$$\boldsymbol{Q}_{\bar{\gamma}'\bar{\gamma}'} = (Q_g - 2Q_h + Q_\iota)\boldsymbol{I}_M + (Q_h - Q_\iota)\boldsymbol{R}^T\boldsymbol{R} + Q_\iota \boldsymbol{J}_M. \tag{30}$$

It is this structure that causes the remarkable reduction from a possible $P=N(N+1)/2$ distinct frequencies to just five distinct frequencies for $L=0$ systems [30].

In particular, letting $\boldsymbol{Q}$ be $\boldsymbol{FG}$, the matrix to be diagonalized, or $\boldsymbol{G}$, the matrix required for the normalization condition, Eq. (27) becomes

$$\boldsymbol{FG} = \begin{pmatrix} \tilde{a}\boldsymbol{I}_N + \tilde{b}\boldsymbol{J}_N & \tilde{e}\boldsymbol{R} + \tilde{f}\boldsymbol{J}_{NM} \\ \tilde{c}\boldsymbol{R}^T + \tilde{d}\boldsymbol{J}_{MN} & \tilde{g}\boldsymbol{I}_M + \tilde{h}\boldsymbol{R}^T\boldsymbol{R} + \tilde{\iota}\boldsymbol{J}_M \end{pmatrix},$$

$$\text{or} \quad \boldsymbol{G} = \begin{pmatrix} \tilde{a}'\boldsymbol{I}_N & \boldsymbol{0} \\ \boldsymbol{0} & \tilde{g}'\boldsymbol{I}_M + \tilde{h}'\boldsymbol{R}^T\boldsymbol{R} \end{pmatrix}, \tag{31}$$

where the coefficients $\tilde{a}$, $\tilde{b}$, $\tilde{c}$, $\tilde{d}$, $\tilde{e}$, $\tilde{f}$, $\tilde{g}$, $\tilde{h}$, and $\tilde{\iota}$ have a simple relation to the elements of the $\boldsymbol{F}$ and $\boldsymbol{G}$ matrices while $\tilde{a}'$, $\tilde{g}'$, and $\tilde{h}'$ have a simple relation to the elements of the $\boldsymbol{G}$ matrix (see Paper I). These coefficients also depend on the choice of $\kappa(D)$ (see Ref. [13]).

B. Symmetry coordinates, normal coordinates, and the Jacobian-weighted wave function

As discussed in Paper I the $\boldsymbol{FG}$ matrix is a $N(N+1)/2\times N(N+1)/2$ dimensional matrix [there being $N(N+1)/2$ internal coordinates], and so the secular equation could have up to $N(N+1)/2$ distinct frequencies. However, as noted above, there are only five distinct frequencies. The S_N symmetry is responsible for the remarkable reduction from $N(N+1)/2$ possible distinct frequencies to five actual distinct

frequencies. As we shall also see, the S_N symmetry greatly simplifies the determination of the normal coordinates and hence the solution of the large-D problem.

The $\boldsymbol{Q}$ matrices, and in particular the $\boldsymbol{FG}$ matrix, are invariants under S_N, so they do not connect subspaces belonging to different irreducible representations of S_N [31]. Thus from Eqs. (22) and (23) the normal coordinates must transform under irreducible representations of S_N. Since the normal coordinates will be linear combinations of the elements of the internal coordinate displacement vectors $\bar{\boldsymbol{r}}'$ and $\bar{\boldsymbol{\gamma}}'$, we first look at the S_N transformation properties of the internal coordinates.

The internal coordinate displacement vectors $\bar{\boldsymbol{r}}'$ and $\bar{\boldsymbol{\gamma}}'$ of Eqs. (17) are basis functions which transform under matrix representations of S_N, and each span the corresponding carrier spaces, however, these representations of S_N are not irreducible representations of S_N.

In Sec. VI A of Paper I we have shown that the reducible representation under which $\bar{\boldsymbol{r}}'$ transforms is reducible to one one-dimensional irreducible representation labeled by the partition $[N]$ [the partition denotes a corresponding Young diagram (=Young pattern=Young shape)] of an irreducible representation (see Appendix C of Paper I) and one $(N-1)$-dimensional irreducible representation labeled by the partition $[N-1,1]$. We will also show that the reducible representation under which $\bar{\boldsymbol{\gamma}}'$ transforms is reducible to one one-dimensional irreducible representation labeled by the partition $[N]$, one $(N-1)$-dimensional irreducible representation labeled by the partition $[N-1,1]$, and one $N(N-3)/2$-dimensional irreducible representation labeled by the partition $[N-2,2]$. Thus if d_α is the dimensionality of the irreducible representation of S_N denoted by the partition α then $d_{[N]}=1$, $d_{[N-1,1]}=N-1$, and $d_{[N-2,2]}=N(N-3)/2$. We note that $d_{[N]}+d_{[N-1,1]}=N$, giving correctly the dimension of the $\bar{\boldsymbol{r}}'$ vector, and that $d_{[N]}+d_{[N-1,1]}+d_{[N-2,2]}=N(N-1)/2$, giving correctly the dimension of the $\bar{\boldsymbol{\gamma}}'$ vector.

Since the normal modes transform under irreducible representations of S_N and are composed of linear combinations of the elements of the internal coordinate displacement vectors $\bar{\boldsymbol{r}}'$ and $\bar{\boldsymbol{\gamma}}'$, there will be two one-dimensional irreducible representations labeled by the partition $[N]$, two $(N-1)$-dimensional irreducible representations labeled by the partition $[N-1,1]$, and one entirely angular $N(N-3)/2$-dimensional irreducible representation labeled by the partition $[N-2,2]$. Thus if we look at Eq. (26) we see that the $\mathbf{0}^{\pm}$ normal modes transform under two $[N]$ irreducible representations, the $\mathbf{1}^{\pm}$ normal modes transform under two $[N-1,1]$ irreducible representations, while the $\mathbf{2}$ normal modes transform under the $[N-2,2]$ irreducible representation.

The wave function for the harmonic-order Hamiltonian of Eq. (21) is thus the product of $P=N(N+1)/2$ harmonic-oscillator wave functions:

$$\Phi_0(\bar{\mathbf{y}}') = \prod_{\mu=\{\mathbf{0}^{\pm},\mathbf{1}^{\pm},\mathbf{2}\}} \prod_{\xi=1}^{d_\mu} \phi_{n_{\mu_\xi}}(\sqrt{\bar{\omega}_\mu}[\boldsymbol{q}'^{\mu}]_\xi), \tag{32}$$

where $\phi_{n_{\mu_\xi}}(\sqrt{\bar{\omega}_\mu}[\boldsymbol{q}'^{\mu}]_\xi)$ is a one-dimensional harmonic-oscillator wave function of frequency $\bar{\omega}_\mu$ and n_{μ_ξ} is the oscillator quantum number, $0 \leqslant n_{\mu_\xi} < \infty$, which counts the number of quanta in each normal mode. The quantity μ labels the manifold of normal modes with the same frequency $\bar{\omega}_\mu$ while $d_\mu=1$, $N-1$ or $N(N-3)/2$ for $\mu=\mathbf{0}^{\pm}$, $\mathbf{1}^{\pm}$, or $\mathbf{2}$, respectively.

VII. CALCULATING THE NORMAL-MODE COORDINATES

In Paper I, we extended previous work to the calculation of the normal coordinates. We summarize this work below in two steps:

(i) In Paper I we have determined two sets of linear combinations of the elements of coordinate vector $\bar{\boldsymbol{r}}'$ which transform under particular orthogonal $[N]$ and $[N-1,1]$ irreducible representations of S_N. These are the symmetry coordinates for the $\bar{\boldsymbol{r}}'$ sector of the problem [19]. Using these two sets of coordinates we then determined two sets of linear combinations of the elements of coordinate vector $\bar{\boldsymbol{\gamma}}'$ which transform under exactly the same orthogonal $[N]$ and $[N-1,1]$ irreducible representations of S_N as the coordinate sets in the $\bar{\boldsymbol{r}}'$ sector was determined. Then another set of linear combinations of the elements of coordinate vector $\bar{\boldsymbol{\gamma}}'$, which transforms under a particular orthogonal $[N-2,2]$ irreducible representation of S_N, was determined. These are then the symmetry coordinates for the $\bar{\boldsymbol{\gamma}}'$ sector of the problem [19]. Furthermore, we chose one of the symmetry coordinates to have the simplest functional form possible under the requirement that it transforms irreducibly under S_N. The succeeding symmetry coordinate was then chosen to have the next simplest functional form possible under the requirement that it transforms irreducibly under S_N, and so on. In this way the complexity of the functional form of the symmetry coordinates has been kept to a minimum and only builds up slowly as more symmetry coordinates of a given species were considered.

(ii) The $\boldsymbol{FG}$ matrix is expressed in the $\bar{\boldsymbol{r}}'$, $\bar{\boldsymbol{\gamma}}'$ basis. However, if we change the basis in which the $\boldsymbol{FG}$ matrix is expressed to the symmetry coordinates an enormous simplification occurs. The $N(N+1)/2 \times N(N+1)/2$ eigenvalue equation of Eq. (23) is reduced to one 2×2 eigenvalue equation for the $[N]$ sector, $N-1$ identical 2×2 eigenvalue equations for the $[N-1,1]$ sector and $N(N-3)/2$ identical 1×1 eigenvalue equations for the $[N-2,2]$ sector. In the case of the 2×2 eigenvalue equations for the $[N]$ and $[N-1,1]$ sectors, the 2×2 structure allows for the mixing in the normal coordinates of the symmetry coordinates in the $\bar{\boldsymbol{r}}'$ and $\bar{\boldsymbol{\gamma}}'$ sectors. The 1×1 structure of the eigenvalue equations in the $[N-2,2]$ sector reflects the fact that there are no $[N-2,2]$ symmetry coordinates in the $\bar{\boldsymbol{r}}'$ sector for the $[N-2,2]$ symmetry coordinates in the $\bar{\boldsymbol{\gamma}}'$ sector to couple with. The $[N-2,2]$ normal modes are entirely angular.

A. Transformation to symmetry coordinates

Let the symmetry coordinate vector $\boldsymbol{S}$ be

$$\boldsymbol{S} = \begin{pmatrix} \boldsymbol{S}_{\bar{\boldsymbol{r}}'}^{[N]} \\ \hline \boldsymbol{S}_{\bar{\boldsymbol{\gamma}}'}^{[N]} \\ \hline \boldsymbol{S}_{\bar{\boldsymbol{r}}'}^{[N-1,1]} \\ \boldsymbol{S}_{\bar{\boldsymbol{\gamma}}'}^{[N-1,1]} \\ \hline \boldsymbol{S}_{\bar{\boldsymbol{\gamma}}'}^{[N-2,2]} \end{pmatrix} = \begin{pmatrix} \boldsymbol{S}^{[N]} \\ \boldsymbol{S}^{[N-1,1]} \\ \boldsymbol{S}^{[N-2,2]} \end{pmatrix}. \tag{33}$$

In $\boldsymbol{S}$, symmetry coordinates of the same species are grouped together. From Paper I we have

$$\boldsymbol{S}_{\bar{\boldsymbol{r}}'}^{[N]} = \frac{1}{\sqrt{N}} \sum_{i=1}^{N} \bar{r}_i', \tag{34}$$

$$\boldsymbol{S}_{\bar{\boldsymbol{\gamma}}'}^{[N]} = \sqrt{\frac{2}{N(N-1)}} \sum_{j=2}^{N} \sum_{i<j} \bar{\gamma}_{ij}', \quad \text{and}$$

$$[\boldsymbol{S}_{\bar{\boldsymbol{r}}'}^{[N-1,1]}]_i = \frac{1}{\sqrt{i(i+1)}} \left(\sum_{k=1}^{i} \bar{r}_k' - i\bar{r}_{i+1}' \right),$$

$$\text{where } 1 \leqslant i \leqslant N-1. \tag{35}$$

We see from Eq. (35) the first symmetry coordinate is proportional to $\bar{r}_1' - \bar{r}_2'$. This involves only the first two particles in the simplest motion possible under the requirement that the symmetry coordinate transforms irreducibly under the $[N-1,1]$ representation of S_N. We again advert that adding another particle to the system does not cause widespread disruption to the symmetry coordinates. The symmetry coordinates, and the motions they describe, remain the same except for an additional symmetry coordinate which describes a motion involving all of the particles.

Again according to item (i) above, $\boldsymbol{S}_{\bar{\boldsymbol{\gamma}}'}^{[N-1,1]}$ should transform under exactly the same nonorthogonal irreducible $[N-1,1]$ representation of S_N as $\boldsymbol{S}_{\bar{\boldsymbol{r}}'}^{[N-1,1]}$. From Paper I

$$\begin{aligned} [\boldsymbol{S}_{\bar{\boldsymbol{\gamma}}'}^{[N-1,1]}]_i &= \frac{1}{\sqrt{i(i+1)(N-2)}} \left(\sum_{k=1}^{i} \sum_{l=1}^{N} \bar{\gamma}_{kl}' - i \sum_{l=1}^{N} \bar{\gamma}_{i+1,l}' \right) \\ &= \frac{1}{\sqrt{i(i+1)(N-2)}} \left(\left[\sum_{l=2}^{i} \sum_{k=1}^{l-1} \bar{\gamma}_{kl}' + \sum_{k=1}^{i} \sum_{l=k+1}^{N} \bar{\gamma}_{kl}' \right] \right. \\ &\quad \left. - i \left[\sum_{k=1}^{i} \bar{\gamma}_{k,i+1}' + \sum_{l=i+2}^{N} \bar{\gamma}_{i+1,l}' \right] \right), \end{aligned} \tag{36}$$

where $1 \leqslant i \leqslant N-1$. Now there is only one sector, the $\bar{\boldsymbol{\gamma}}'$ sector, belonging to the $[N-2,2]$ species. From Paper I

$$\begin{aligned} [\boldsymbol{S}_{\bar{\boldsymbol{\gamma}}'}^{[N-2,2]}]_{ij} &= \frac{1}{\sqrt{i(i+1)(j-3)(j-2)}} \left(\sum_{j'=2}^{j-1} \sum_{k=1}^{[j'-1,i]_{min}} \bar{\gamma}_{kj'}' \right. \\ &\quad + \sum_{k=1}^{i-1} \sum_{j'=k+1}^{i} \bar{\gamma}_{kj'}' - (j-3) \sum_{k=1}^{i} \bar{\gamma}_{kj}' - i \sum_{k=1}^{i} \bar{\gamma}_{k,(i+1)}' \\ &\quad \left. - i \sum_{j'=i+2}^{j-1} \bar{\gamma}_{(i+1),j'}' + i(j-3) \bar{\gamma}_{(i+1),j}' \right), \end{aligned} \tag{37}$$

where $1 \leqslant i \leqslant j-2$ and $4 \leqslant j \leqslant N$.

This fulfills item (i) above: the determination of the symmetry coordinates.

B. Transformation to normal-mode coordinates

In Paper I we apply the ***FG*** method using these symmetry coordinates to determine the frequencies and normal modes of the system:

$$\lambda_\alpha^{\pm} = \frac{a_\alpha \pm \sqrt{b_\alpha^2 + 4c_\alpha}}{2} \tag{38}$$

for the $\alpha = [N]$ and $[N-1,1]$ sectors, where

$$a_\alpha = [\boldsymbol{\sigma}_{\boldsymbol{\alpha}}^{\boldsymbol{FG}}]_{\bar{\boldsymbol{r}}',\bar{\boldsymbol{r}}'} + [\boldsymbol{\sigma}_{\boldsymbol{\alpha}}^{\boldsymbol{FG}}]_{\bar{\boldsymbol{\gamma}}',\bar{\boldsymbol{\gamma}}'}$$

$$b_\alpha = [\boldsymbol{\sigma}_{\boldsymbol{\alpha}}^{\boldsymbol{FG}}]_{\bar{\boldsymbol{r}}',\bar{\boldsymbol{r}}'} - [\boldsymbol{\sigma}_{\boldsymbol{\alpha}}^{\boldsymbol{FG}}]_{\bar{\boldsymbol{\gamma}}',\bar{\boldsymbol{\gamma}}'}$$

$$c_\alpha = [\boldsymbol{\sigma}_{\boldsymbol{\alpha}}^{\boldsymbol{FG}}]_{\bar{\boldsymbol{r}}',\bar{\boldsymbol{\gamma}}'} \times [\boldsymbol{\sigma}_{\boldsymbol{\alpha}}^{\boldsymbol{FG}}]_{\bar{\boldsymbol{\gamma}}',\bar{\boldsymbol{r}}'}, \tag{39}$$

while $\lambda_{[N-2,2]} = \boldsymbol{\sigma}_{[\boldsymbol{N-2,2}]}^{\boldsymbol{FG}}$. The $\boldsymbol{\sigma}_{\boldsymbol{\alpha}}^{\boldsymbol{FG}}$ are related to the $\tilde{a}$, $\tilde{b}$, $\tilde{c}$, $\tilde{d}$, $\tilde{e}$, $\tilde{f}$, $\tilde{g}$, $\tilde{h}$, and $\tilde{\iota}$ of the ***FG*** matrix of Eq. (31). Note that the $\boldsymbol{\sigma}_{\boldsymbol{\alpha}}^{\boldsymbol{FG}}$ for the $\alpha = [N]$ and $[N-1,1]$ sectors are 2×2 matrices while $\boldsymbol{\sigma}_{[\boldsymbol{N-2,2}]}^{\boldsymbol{FG}}$ is a one-component quantity.

The normal coordinates are given by

$$\boldsymbol{q}_{\pm}'^{\alpha} = c_{\pm}^{\alpha} (\cos\theta_{\pm}^{\alpha} [\boldsymbol{S}_{\bar{\boldsymbol{r}}'}^{\alpha}]_\xi + \sin\theta_{\pm}^{\alpha} [\boldsymbol{S}_{\bar{\boldsymbol{\gamma}}'}^{\alpha}]_\xi) \tag{40}$$

for the $\alpha = [N]$ and $[N-1,1]$ sectors, and

$$\boldsymbol{q}'^{[N-2,2]} = c^{[N-2,2]} \boldsymbol{S}_{\bar{\boldsymbol{\gamma}}'}^{[N-2,2]}. \tag{41}$$

The $\bar{\boldsymbol{r}}'$-$\bar{\boldsymbol{\gamma}}'$ mixing angle, $\theta_{\pm}^{\alpha}$, is given by

$$\tan\theta_{\pm}^{\alpha} = \frac{(\lambda_\alpha^{\pm} - [\boldsymbol{\sigma}_{\boldsymbol{\alpha}}^{\boldsymbol{FG}}]_{\bar{\boldsymbol{r}}',\bar{\boldsymbol{r}}'})}{[\boldsymbol{\sigma}_{\boldsymbol{\alpha}}^{\boldsymbol{FG}}]_{\bar{\boldsymbol{r}}',\bar{\boldsymbol{\gamma}}'}} = \frac{[\boldsymbol{\sigma}_{\boldsymbol{\alpha}}^{\boldsymbol{FG}}]_{\bar{\boldsymbol{\gamma}}',\bar{\boldsymbol{r}}'}}{(\lambda_\alpha^{\pm} - [\boldsymbol{\sigma}_{\boldsymbol{\alpha}}^{\boldsymbol{FG}}]_{\bar{\boldsymbol{\gamma}}',\bar{\boldsymbol{\gamma}}'})}, \tag{42}$$

while the normalization constants c are given by

$$c_{\pm}^{\alpha} = \frac{1}{\sqrt{\begin{pmatrix} \cos\theta_{\pm}^{\alpha} \\ \sin\theta_{\pm}^{\alpha} \end{pmatrix}^T \boldsymbol{\sigma}_{\boldsymbol{\alpha}}^{\boldsymbol{G}} \begin{pmatrix} \cos\theta_{\pm}^{\alpha} \\ \sin\theta_{\pm}^{\alpha} \end{pmatrix}}} \quad \text{and} \quad c^{[N-2,2]} = \frac{1}{\sqrt{\boldsymbol{\sigma}_{[\boldsymbol{N-2,2}]}^{\boldsymbol{G}}}}. \tag{43}$$

The $\boldsymbol{\sigma}_{\boldsymbol{\alpha}}^{\boldsymbol{G}}$ are related to the $\tilde{a}'$, $\tilde{g}'$, and $\tilde{h}'$ of the ***G*** matrix of Eq. (31).

This fulfills item (ii) above: the determination of the

frequencies and normal coordinates. Equations (40) and (41) represent the final results of Paper I, the normal coordinates.

VIII. DERIVING THE DENSITY PROFILE OF A BEC FROM THE WAVE FUNCTION

As a first application of this general theory from Paper I, we calculate the density profile for a confined quantum system. The harmonic-order DPT wave function, ${}_g\Phi_0(\bar{\mathbf{y}}')$, for the ground state is given by Eq. (32) with all of the n_{μ_ξ} set equal to zero, i.e.,

$$ {}_g\Phi_0(\bar{\mathbf{y}}') = \prod_{\mu=\{\mathbf{0}^\pm,\mathbf{1}^\pm,\mathbf{2}\}} \prod_{\xi=1}^{d_\mu} \phi_0(\sqrt{\bar{\omega}_\mu}[\boldsymbol{q}'^\mu]_\xi), \tag{44}$$

where

$$ \phi_0(\sqrt{\bar{\omega}_\mu}[\boldsymbol{q}'^\mu]_\xi) = \left(\frac{\bar{\omega}_\mu}{\pi}\right)^{1/4} \exp\left(-\frac{1}{2}\bar{\omega}_\mu[\boldsymbol{q}'^\mu]_\xi^2\right). \tag{45}$$

Now the ground-state wave function of a BEC is completely symmetric under interchange of any of the particles and so we require ${}_g\Phi_0(\bar{\mathbf{y}}')$ of Eq. (44) to be completely symmetric under interchange of any of the particles. This follows from the fact that the five $\Pi_{\xi=1}^{d_\mu}\phi_0(\sqrt{\bar{\omega}_\mu}[\boldsymbol{q}'^\mu]_\xi)$, where $\mu=\{\mathbf{0}^\pm,\mathbf{1}^\pm,\mathbf{2}\}$, are each completely symmetric under interchange of any of the particles. This may be seen from the fact that

$$ \prod_{\xi=1}^{d_\mu} \phi_0(\sqrt{\bar{\omega}_\mu}[\boldsymbol{q}'^\mu]_\xi) = \left(\sqrt{\frac{\bar{\omega}_\mu}{\pi}}\right)^{d_\mu} \exp\left(-\frac{1}{2}\bar{\omega}_\mu\left\{\sum_{\xi=1}^{d_\mu}[\boldsymbol{q}'^\mu]_\xi^2\right\}\right). \tag{46}$$

Now according to items (i) and (ii) of Sec. VII, particle interchange is effected by orthogonal transformations of the $[\boldsymbol{q}'^\mu]_\xi$, where $1\leqslant\xi\leqslant d_\mu$, and any orthogonal transformation leaves $\Sigma_{\xi=1}^{d_\mu}[\boldsymbol{q}'^\mu]_\xi^2$ invariant. Together with Eq. (46), this fact means that the $\Pi_{\xi=1}^{d_\mu}\phi_0(\sqrt{\bar{\omega}_\mu}[\boldsymbol{q}'^\mu]_\xi)$ are completely symmetric under interchange of any of the particles as advertised.

Defining $S(D)$ to be the total D-dimensional solid angle [32],

$$ S(D) = \frac{2\pi^{D/2}}{\Gamma\left(\frac{D}{2}\right)}, \tag{47}$$

where we note that $S(1)=2$, $S(2)=2\pi$, $S(3)=4\pi$, $S(4)=2\pi^2,\ldots$, the harmonic-order Jacobian-weighted ground-state density profile $N_0(r)$ is

$$ \begin{aligned} S(D)N_0(r) &= S(D)r^{(D-1)}\rho_0(r) \\ &= \sum_{i=1}^{N}\int_{-\infty}^{\infty}\cdots\int_{-\infty}^{\infty}\delta_f(r-r_i) \\ &\quad\times[{}_g\Phi_0(\bar{\mathbf{y}}')]^2\prod_{\mu=\mathbf{0}^\pm,\mathbf{1}^\pm,\mathbf{2}}\prod_{\xi=1}^{d_\mu} d[\boldsymbol{q}'^\mu]_\xi, \end{aligned} \tag{48}$$

where $\rho_0(r)$ is the unweighted harmonic-order ground-state density profile and $\delta_f(r-r_i)$ is the Dirac delta function and is differentiated from the inverse dimension δ by the subscript f. Since ${}_g\Phi_0(\bar{\mathbf{y}}')$ is invariant under particle interchange then

$$ \begin{aligned} S(D)N_0(r) &= N\int_{-\infty}^{\infty}\cdots\int_{-\infty}^{\infty}\delta_f(r-r_N) \\ &\quad\times[{}_g\Phi_0(\bar{\mathbf{y}}')]^2\prod_{\mu=\mathbf{0}^\pm,\mathbf{1}^\pm,\mathbf{2}}\prod_{\xi=1}^{d_\mu} d[\boldsymbol{q}'^\mu]_\xi. \end{aligned} \tag{49}$$

Upon using Eq. (44) and the fact that r_N only appears in $\boldsymbol{q}'^{\mathbf{0}^+}$, $\boldsymbol{q}'^{\mathbf{0}^-}$, $[\boldsymbol{q}'^{\mathbf{1}^+}]_{d_{\mathbf{1}^+}}$, and $[\boldsymbol{q}'^{\mathbf{1}^-}]_{d_{\mathbf{1}^-}}$ [see Eqs. (9), (17), (34)–(37), (40), and (41) and Eq. (45)] we obtain

$$ \begin{aligned} S(D)N_0(r) &= N\int_{-\infty}^{\infty}\int_{-\infty}^{\infty}\int_{-\infty}^{\infty}\int_{-\infty}^{\infty}\delta_f(r-r_N) \\ &\quad\times\prod_{\mu=\mathbf{0}^\pm,\mathbf{1}^\pm}[\phi_0(\sqrt{\bar{\omega}_\mu}[\boldsymbol{q}'^\mu]_{d_\mu})]^2 d[\boldsymbol{q}'^\mu]_{d_\mu} \\ &= \frac{N\sqrt{\bar{\omega}_{\mathbf{0}^+}\bar{\omega}_{\mathbf{0}^-}\bar{\omega}_{\mathbf{1}^+}\bar{\omega}_{\mathbf{1}^-}}}{\pi^2}\int_{-\infty}^{\infty}\int_{-\infty}^{\infty}\int_{-\infty}^{\infty}\int_{-\infty}^{\infty}\delta_f(r-r_N) \\ &\quad\times\exp\left(-\sum_{\nu=\mathbf{0}^\pm,\mathbf{1}^\pm}\bar{\omega}_\nu[\boldsymbol{q}'^\nu]_{d_\nu}^2\right)\prod_{\zeta=\mathbf{0}^\pm,\mathbf{1}^\pm} d[\boldsymbol{q}'^\zeta]_{d_\zeta}. \end{aligned} \tag{50}$$

The delta function, $\delta_f(r-r_N)$, is a function of r_N while the integral is over the normal coordinates $\boldsymbol{q}'^{\mathbf{0}^+}$, $\boldsymbol{q}'^{\mathbf{0}^-}$, $[\boldsymbol{q}'^{\mathbf{1}^+}]_{N-1}$, and $[\boldsymbol{q}'^{\mathbf{1}^-}]_{N-1}$. Thus we need a change of variables to perform the integral. We change the variables of the integral to $\bar{r}'_N$, $\bar{r}'_S$, $\boldsymbol{S}^{[N]}_{\bar{\boldsymbol{\gamma}}'}$, and $[\boldsymbol{S}^{[N-1,1]}_{\bar{\boldsymbol{\gamma}}'}]_{(N-1)}$, where

$$ \bar{r}'_S = \sum_{i=1}^{N-1}\bar{r}'_i, \tag{51}$$

$\boldsymbol{S}^{[N]}_{\bar{\boldsymbol{\gamma}}'}$ is given by Eq. (34) and $[\boldsymbol{S}^{[N-1,1]}_{\bar{\boldsymbol{\gamma}}'}]_{(N-1)}$ is given by Eq. (36). Thus from Eqs. (35), (40), (41), and (51) we obtain

$$ \begin{pmatrix} \boldsymbol{q}'^{\mathbf{0}^+} \\ \boldsymbol{q}'^{\mathbf{0}^-} \\ [\boldsymbol{q}'^{\mathbf{1}^+}]_{N-1} \\ [\boldsymbol{q}'^{\mathbf{1}^-}]_{N-1} \end{pmatrix} = \boldsymbol{T}\boldsymbol{a}', \tag{52}$$

where

$$ \boldsymbol{a}' = \begin{pmatrix} \bar{r}'_N \\ \bar{r}'_S \\ \boldsymbol{S}^{[N]}_{\bar{\boldsymbol{\gamma}}'} \\ [\boldsymbol{S}^{[N-1,1]}_{\bar{\boldsymbol{\gamma}}'}]_{(N-1)} \end{pmatrix}, $$

$$\boldsymbol{T} = \begin{pmatrix} T_{11} & T_{11} & T_{13} & 0 \\ T_{21} & T_{21} & T_{23} & 0 \\ -(N-1)T_{31} & T_{31} & 0 & T_{34} \\ -(N-1)T_{41} & T_{41} & 0 & T_{44} \end{pmatrix}, \tag{53}$$

and

$$T_{11} = \frac{c_+^{[N]} \cos\theta_+^{[N]}}{\sqrt{N}}, \quad T_{13} = c_+^{[N]} \sin\theta_+^{[N]},$$

$$T_{21} = \frac{c_-^{[N]} \cos\theta_-^{[N]}}{\sqrt{N}}, \quad T_{23} = c_-^{[N]} \sin\theta_-^{[N]},$$

$$T_{31} = \frac{c_+^{[N-1,1]} \cos\theta_+^{[N-1,1]}}{\sqrt{N(N-1)}}, \quad T_{34} = c_+^{[N-1,1]} \sin\theta_+^{[N-1,1]},$$

$$T_{41} = \frac{c_-^{[N-1,1]} \cos\theta_-^{[N-1,1]}}{\sqrt{N(N-1)}}, \quad T_{44} = c_-^{[N-1,1]} \sin\theta_-^{[N-1,1]}. \tag{54}$$

The Jacobian J_T of the transformation is thus

$$J_T = \det T = -\frac{c_+^{[N]} c_-^{[N]} c_+^{[N-1,1]} c_-^{[N-1,1]}}{\sqrt{N-1}} \times \sin(\theta_+^{[N]} - \theta_-^{[N]}) \sin(\theta_+^{[N-1,1]} - \theta_-^{[N-1,1]}). \tag{55}$$

Defining

$$\bar{\boldsymbol{\Omega}} = \begin{pmatrix} \bar{\omega}_{\mathbf{0}^+} & 0 & 0 & 0 \\ 0 & \bar{\omega}_{\mathbf{0}^-} & 0 & 0 \\ 0 & 0 & \bar{\omega}_{\mathbf{1}^+} & 0 \\ 0 & 0 & 0 & \bar{\omega}_{\mathbf{1}^-} \end{pmatrix} \tag{56}$$

then

$$S(D)N_0(r) = \frac{NJ_T\sqrt{\bar{\omega}_{\mathbf{0}^+}\bar{\omega}_{\mathbf{0}^-}\bar{\omega}_{\mathbf{1}^+}\bar{\omega}_{\mathbf{1}^-}}}{\pi^2} \int_{-\infty}^{\infty}\int_{-\infty}^{\infty}\int_{-\infty}^{\infty}\int_{-\infty}^{\infty} \delta_f(r - r_N) \times \exp(-\boldsymbol{a}'^T \boldsymbol{T}^T \bar{\boldsymbol{\Omega}} \boldsymbol{T} \boldsymbol{a}') d\bar{r}_N' \, d^3\boldsymbol{b}', \tag{57}$$

where $d^3\boldsymbol{b}' = d\bar{r}_S' d\boldsymbol{S}_{\bar{\gamma}'}^{[N]} d[\boldsymbol{S}_{\bar{\gamma}'}^{[N-1,1]}]_{(N-1)}$. Writing

$$\boldsymbol{T}^T \bar{\boldsymbol{\Omega}} \boldsymbol{T} = \begin{pmatrix} K_0 & \boldsymbol{K}^T \\ \boldsymbol{K} & \boldsymbol{\mathcal{K}} \end{pmatrix}, \tag{58}$$

where

$$K_0 = \bar{\omega}_{\mathbf{0}^+} T_{11}^2 + \bar{\omega}_{\mathbf{0}^-} T_{21}^2 + (N-1)^2(\bar{\omega}_{\mathbf{1}^+} T_{31}^2 + \bar{\omega}_{\mathbf{1}^-} T_{41}^2), \tag{59}$$

$$\boldsymbol{K} = \begin{pmatrix} \bar{\omega}_{\mathbf{0}^+} T_{11}^2 + \bar{\omega}_{\mathbf{0}^-} T_{21}^2 - (N-1)(\bar{\omega}_{\mathbf{1}^+} T_{31}^2 + \bar{\omega}_{\mathbf{1}^-} T_{41}^2) \\ \bar{\omega}_{\mathbf{0}^+} T_{11} T_{13} + \bar{\omega}_{\mathbf{0}^-} T_{21} T_{23} \\ -(N-1)(\bar{\omega}_{\mathbf{1}^+} T_{31} T_{34} + \bar{\omega}_{\mathbf{1}^-} T_{41} T_{44}) \end{pmatrix}, \tag{60}$$

$$\boldsymbol{\mathcal{K}}_{11} = \bar{\omega}_{\mathbf{0}^+} T_{11}^2 + \bar{\omega}_{\mathbf{0}^-} T_{21}^2 + \bar{\omega}_{\mathbf{1}^+} T_{31}^2 + \bar{\omega}_{\mathbf{1}^-} T_{41}^2,$$

$$\boldsymbol{\mathcal{K}}_{12} = \boldsymbol{\mathcal{K}}_{21} = \bar{\omega}_{\mathbf{0}^+} T_{11} T_{13} + \bar{\omega}_{\mathbf{0}^-} T_{21} T_{23},$$

$$\boldsymbol{\mathcal{K}}_{13} = \boldsymbol{\mathcal{K}}_{31} = \bar{\omega}_{\mathbf{1}^+} T_{31} T_{34} + \bar{\omega}_{\mathbf{1}^-} T_{41} T_{44},$$

$$\boldsymbol{\mathcal{K}}_{22} = \bar{\omega}_{\mathbf{0}^+} T_{13}^2 + \bar{\omega}_{\mathbf{0}^-} T_{23}^2,$$

$$\boldsymbol{\mathcal{K}}_{23} = \boldsymbol{\mathcal{K}}_{32} = 0, \quad \boldsymbol{\mathcal{K}}_{33} = \bar{\omega}_{\mathbf{1}^+} T_{34}^2 + \bar{\omega}_{\mathbf{1}^-} T_{44}^2. \tag{61}$$

Using Eqs. (53) and (58) in Eq. (57), we obtain

$$S(D)N_0(r) = \frac{NJ_T\sqrt{\bar{\omega}_{\mathbf{0}^+}\bar{\omega}_{\mathbf{0}^-}\bar{\omega}_{\mathbf{1}^+}\bar{\omega}_{\mathbf{1}^-}}}{\pi^2} \int_{-\infty}^{\infty}\int_{-\infty}^{\infty}\int_{-\infty}^{\infty}\int_{-\infty}^{\infty} \delta_f(r - r_N) \times \exp(-K_0 \bar{r}_N'^2 - 2\bar{r}_N' \boldsymbol{K}^T \boldsymbol{b}' - \boldsymbol{b}'^T \boldsymbol{\mathcal{K}} \boldsymbol{b}') d\bar{r}_N' d^3\boldsymbol{b}', \tag{62}$$

where

$$\boldsymbol{b}' = \begin{pmatrix} \bar{r}_S' \\ \boldsymbol{S}_{\bar{\gamma}'}^{[N]} \\ [\boldsymbol{S}_{\bar{\gamma}'}^{[N-1,1]}]_{(N-1)} \end{pmatrix}. \tag{63}$$

Since $\delta_f(r - r_N) = \sqrt{\delta}\kappa(D)\delta_f\left[\delta^{-1/2}\left(\frac{r}{\kappa(D)} - \bar{r}_\infty\right) - \bar{r}_N'\right]$, then

$$S(D)N_0(r) = \frac{NJ_T\sqrt{\delta}\kappa(D)\sqrt{\bar{\omega}_{\mathbf{0}^+}\bar{\omega}_{\mathbf{0}^-}\bar{\omega}_{\mathbf{1}^+}\bar{\omega}_{\mathbf{1}^-}}}{\pi^2} \times \int_{-\infty}^{\infty}\int_{-\infty}^{\infty}\int_{-\infty}^{\infty} \exp\left[-\delta^{-1} K_0\left(\frac{r}{\kappa(D)} - \bar{r}_\infty\right)^2 - 2\delta^{-1/2}\left(\frac{r}{\kappa(D)} - \bar{r}_\infty\right)\boldsymbol{K}^T \boldsymbol{b}' - \boldsymbol{b}'^T \boldsymbol{\mathcal{K}} \boldsymbol{b}'\right] d^3\boldsymbol{b}'. \tag{64}$$

Using

$$\int_{-\infty}^{\infty} \cdots \int_{-\infty}^{\infty} \exp(-\boldsymbol{b}'^T \boldsymbol{A} \boldsymbol{b}' - 2\boldsymbol{B}^T \boldsymbol{b}') d^n\boldsymbol{b}' = \frac{\pi^{n/2}}{\sqrt{\det \boldsymbol{A}}} \exp(\boldsymbol{B}^T \boldsymbol{A}^{-1} \boldsymbol{B}), \tag{65}$$

Eq. (64) yields

$$S(D)N_0(r) = \frac{N\sqrt{\delta}\kappa(D)}{\sqrt{\pi}} \sqrt{\frac{\bar{\omega}_{\mathbf{0}^+}\bar{\omega}_{\mathbf{0}^-}\bar{\omega}_{\mathbf{1}^+}\bar{\omega}_{\mathbf{1}^-} J_T^2}{\det \boldsymbol{\mathcal{K}}}} \times \exp\left[-\delta^{-1}\left(\frac{r}{\kappa(D)} - \bar{r}_\infty\right)^2 (K_0 - \boldsymbol{K}^T \boldsymbol{\mathcal{K}}^{-1} \boldsymbol{K})\right]. \tag{66}$$

Since

$$\frac{\bar{\omega}_{\mathbf{0}^+}\bar{\omega}_{\mathbf{0}^-}\bar{\omega}_{\mathbf{1}^+}\bar{\omega}_{\mathbf{1}^-} J_T^2}{\det \boldsymbol{\mathcal{K}}} = (K_0 - \boldsymbol{K}^T \boldsymbol{\mathcal{K}}^{-1} \boldsymbol{K}), \tag{67}$$

then

$$S(D)N_0(r) = N\sqrt{\frac{\delta\kappa^2(D)(K_0 - \boldsymbol{K}^T\boldsymbol{\mathcal{K}}^{-1}\boldsymbol{K})}{\pi}} \times \exp\left[-\delta^{-1}\left(\frac{r}{\kappa(D)} - \bar{r}_\infty\right)^2 (K_0 - \boldsymbol{K}^T\boldsymbol{\mathcal{K}}^{-1}\boldsymbol{K})\right]. \tag{68}$$

The harmonic-order DPT Jacobian-weighted density profile $N_0(r)$ is correctly normalized to N, since upon using Eq. (65) (with $n=1$, $\boldsymbol{A}=(K_0-\boldsymbol{K}^T\boldsymbol{\mathcal{K}}^{-1}\boldsymbol{K})/[\delta\kappa^2(D)]$ and $\boldsymbol{B}=-\bar{r}_\infty(K_0-\boldsymbol{K}^T\boldsymbol{\mathcal{K}}^{-1}\boldsymbol{K})[\delta_\kappa(D)]$) in Eq. (68) we find

$$\int_\Omega \int_{-\infty}^{\infty} N_0(r)drd\Omega = N. \tag{69}$$

Notice that the harmonic-order DPT density profile is a normalized Gaussian centered around $r=\kappa(D)\bar{r}_\infty$, the $D\to\infty$ configuration radius [see Eqs. (9) and (13)].

IX. OPTIMIZING THE HARMONIC-ORDER RESULT

Let us look in more detail at the harmonic-order wave function. In the notation of Eqs. (16) and (18), Eq. (17) can be written as

$$\bar{\boldsymbol{y}} = \bar{\boldsymbol{y}}_\infty + \delta^{1/2}\bar{\boldsymbol{y}}', \tag{70}$$

where

$$\bar{\boldsymbol{y}}_\infty = \bar{\boldsymbol{y}}\Big|_{\substack{\bar{r}_i=\bar{r}_\infty \\ \bar{\gamma}'_{jk}=\bar{\gamma}'_\infty}} \quad \begin{matrix} \forall \quad 1 \leqslant i \leqslant N \text{ and} \\ 1 \leqslant j < k \leqslant N. \end{matrix} \tag{71}$$

Inserting Eq. (70) into Eq. (22) one obtains $\boldsymbol{q}=\boldsymbol{q}_\infty+\delta^{1/2}\boldsymbol{q}'$, where $\boldsymbol{q}_\infty=\boldsymbol{b}^T\bar{\boldsymbol{y}}_\infty$. Using these in Eq. (32) one obtains

$$\Phi_0(\bar{\boldsymbol{y}}') = \prod_{\mu=\{\boldsymbol{0}^\pm,\boldsymbol{1}^\pm,\boldsymbol{2}\}} \prod_{\xi=1}^{d_\mu} \phi_{n_{\mu_\xi}}[\{D\bar{\omega}_\mu\}^{1/2}([\boldsymbol{q}^\mu]_\xi - \boldsymbol{q}^\mu_\infty)]. \tag{72}$$

Equation (72) represents oscillations about the $D\to\infty$ configuration $\boldsymbol{q}^\mu_\infty$ with frequencies $\{D\bar{\omega}_\mu\}$. For a macroscopic quantum confined system at $\delta=1/3$ $(D=3)$, $D\bar{\omega}_\mu=3\bar{\omega}_\mu$ is sufficiently small that this harmonic-order, Jacobian-weighted wave function has a macroscopic extension. However, when D becomes large (δ becomes small) the frequencies $\{D\bar{\omega}_\mu\}$ becomes very large and so, according to Eq. (72), the harmonic-order wave function becomes strongly localized about $[\boldsymbol{q}^\mu]_\xi=\boldsymbol{q}^\mu_\infty$ (i.e., it features short wavelengths).

This dimensional behavior has interesting, and very useful consequences. As is well known, the energy and density profile of a small-a Bose-Einstein condensate at $D=3$ depends only on the scattering length of the interatomic potential, and not the detailed shape of the potential. This is due to the long-wavelength nature of BEC's: for small to moderate scattering lengths, the atomic wavelengths are not short enough to "resolve" the short-range detail of the potential. However, for large D the atomic wavelengths become very short, since according to Eqs. (9) and (10), the scaled, Jacobian-transformed Hamiltonian displays an effective mass term proportional to D^2. Thus as we have noted above, and unlike at $D=3$, the wavelength of the wave function for the large-D system becomes smaller and becomes sensitive to the details of the potential.

This feature is actually advantageous. A perturbation theory in some parameter which at low orders displays an insensitivity to the precise shape of the interatomic potential could not be optimized to yield results at low order that would be close to the actual results. For example, one could not reasonably expect the energy and density profile at low orders to be both insensitive to the precise shape of the interatomic potential for small fixed scattering length and, at the same time, to differ only a small amount from the actual $D=3$ condensate energy and density profile. The energy and density profile at low orders would almost certainly be different from the actual $D=3$ condensate.

The large-D sensitivity to the details of the interatomic potential in the present method enables us to optimize our dimensional continuation of the interparticle potential so that higher-order contributions of this theory will be small.

X. APPLICATION: THE DENSITY PROFILE FOR AN N-ATOM BOSE-EINSTEIN CONDENSATE

We assume a $T=0$ K condensate which is confined by an isotropic, harmonic trap with frequency ω_{ho}:

$$V_{\text{conf}}(r_i) = \frac{1}{2}m\omega_{ho}^2 r_i^2. \tag{73}$$

A realistic two-body atom-atom interaction potential would lead to a solidlike ground state, and so typically this two-body potential is replaced with a pseudopotential which does not support bound states. We follow most other work and replace the actual atom-atom potential by a hard sphere of radius a:

$$V_{\text{int}}(r_{ij}) = \begin{cases} \infty, & r_{ij} < a \\ 0, & r_{ij} \geqslant a \end{cases}, \tag{74}$$

where a is the s-wave scattering length of the condensate atoms. We dimensionally continue the hard-sphere potential so that it is differentiable away from $D=3$, allowing us to perform the dimensional perturbation analysis (see Refs. [13,14] as well as a later discussion in this paper). Thus we take the interaction to be

$$V_{\text{int}}(r_{ij}) = \frac{V_o}{1-3/D}\left[1 - \tanh\left(\frac{c_o}{1-3/D}(r_{ij}-a)\right)\right], \tag{75}$$

where D is the Cartesian dimensionality of space. This interaction becomes a hard sphere of radius a in the physical, $D=3$, limit. The two constants, V_o and c_o (which determine the height and the slope of the potential) are parameters that allow us to fine-tune the large-D shape of the potential and optimize our results through harmonic order by minimizing the contribution of the higher-order terms beyond harmonic (see Sec. XI). Although we have chosen the simplest possibility for the interatomic potential, two parameters, we can have any number of parameters providing for a more general and flexible potential [14]. The functional form of the potential at $D\neq 3$ is not unique. Other functional forms could be

chosen with equal success as long as the form is differentiable and reduces to a hard-sphere potential at $D=3$. We simply choose a form that allows a gradual softening of the hard wall.

We need to regularize the large-D limit of the Jacobian-weighted Hamiltonian ($J^{1/2}HJ^{-1/2}$). We do this by converting the variables to dimensionally scaled harmonic-oscillator units (bars):

$$\bar{r}_i = \frac{r_i}{D^2 \bar{a}_{ho}}, \quad \bar{E} = \frac{D^2}{\hbar \bar{\omega}_{ho}} E, \quad \bar{H} = \frac{D^2}{\hbar \bar{\omega}_{ho}} H, \quad \bar{a} = \frac{a}{\sqrt{2} D^2 \bar{a}_{ho}},$$

$$\bar{V}_o = \frac{D^2}{\hbar \bar{\omega}_{ho}} V_o, \quad \bar{c}_o = \sqrt{2} D^2 \bar{a}_{ho} c_o, \tag{76}$$

where

$$\bar{a}_{ho} = \sqrt{\frac{\hbar}{m \bar{\omega}_{ho}}} \quad \text{and} \quad \bar{\omega}_{ho} = D^3 \omega_{ho} \tag{77}$$

are the dimensionally scaled harmonic-oscillator length and dimensionally scaled trap frequency, respectively. In this case we have chosen $\kappa(D)=D^2\bar{a}_{\mathrm{ho}}$, while the dimensionally scaled harmonic-oscillator units of energy, length, and time are $\hbar\bar{\omega}_{ho}$, $\bar{a}_{ho}$, and $1/\bar{\omega}_{ho}$, respectively. All barred constants ($\bar{a}$, $\bar{a}_{ho}$, $\bar{\omega}_{ho}$, $\bar{V}_o$, and $\bar{c}_o$) are held fixed as D varies. For example, as D varies $\bar{a}$ is held fixed at a value by requiring that it give the physical unscaled scattering length at $D=3$.

In dimensionally scaled units the total interaction term reads

$$V = V_{\mathrm{conf}} + V_{\mathrm{int}} = \sum_{i=1}^{N} \frac{1}{2} \bar{r}_i^2 + \frac{\bar{V}_o}{1 - 3\delta} \sum_{i=1}^{N} \sum_{j=i+1}^{N} \left\{ 1 - \tanh\left[\frac{\bar{c}_o}{1 - 3\delta} \left(\frac{\bar{r}_{ij}}{\sqrt{2}} - \bar{a} \right) \right] \right\}. \tag{78}$$

The infinite-D ($\delta \to 0$) effective potential in dimensionally scaled harmonic-oscillator units of Eqs. (76) and (77) is

$$V_{\mathrm{eff}} = \sum_{i=1}^{N} \left(\frac{1}{8\bar{r}_i^2} \frac{\Gamma^{(i)}}{\Gamma} + \frac{1}{2} \bar{r}_i^2 \right) + \bar{V}_o \sum_{i=1}^{N} \sum_{j=i+1}^{N} \left\{ 1 - \tanh\left[\bar{c}_o \left(\frac{\bar{r}_{ij}}{\sqrt{2}} - \bar{a} \right) \right] \right\}. \tag{79}$$

One can see from the double-sum term in V_{eff} that the large-D interatomic potential has become a soft sphere of radius $\bar{a}$ and height $2\bar{V}_o$. The slope of the soft wall is determined by $\bar{c}_o$. The development of DPT using the three-parameter extension of Eq. (75) is discussed at length in Ref. [13], while a four-parameter extension of Eq. (75) is discussed in Ref. [14].

As noted above, the two parameters in Eq. (79) are chosen with the goal of minimizing the contribution of the higher-order beyond-harmonic terms, and so optimizing the harmonic-order DPT density profile [of Eq. (68)] and energy perturbation series through harmonic order in δ [Eq. (25)].

XI. OPTIMIZATION OF THE INTERPARTICLE PARAMETERS OF A QUANTUM CONFINED SYSTEM

We consider a BEC in a spherical trap where $\omega_{ho}=2\pi \times 77.87$ Hz and for which $a=1000$ a.u. or $0.0433a_{ho}$ in oscillator units ($a_{ho}=\sqrt{\hbar/m\omega_{ho}}$) which is approximately equal to ten times the natural ^{87}Rb value. We choose this value for the scattering length since the actual density profiles and energies show a noticeable difference from the mean-field, Gross-Pitaevskii (GP) equation result at low N, and yet the modified Gross-Pitaevskii (MGP) equation [33] remains valid for comparison to the DPT result.

The potential is optimized by fitting the energies through harmonic order to benchmark DMC energies [10] at low atom number ($N \leqslant 50$) and DMC density profiles for $N=3$ and $N=10$ (DMC density profiles for larger N have not been obtained [10]). Since in our DPT analysis the number of atoms N is a parameter, we can readily extrapolate to larger N without large amounts of calculation.

A least-squares fit is used to optimize the parameters of the dimensionally continued interatomic potential. We fit to six accurate low-N DMC energies [10] and, as noted above, the position and height of the peak of the DMC density profile for $N=3$ and $N=10$. The DPT values for the position and height of the peak of the density profile are just

$$\bar{r}_{peak}^{(DPT)}(N; \bar{V}_o, \bar{c}_o) = \bar{r}_{\infty} \tag{80}$$

$$(N_0)_{max}^{(DPT)}(N; \bar{V}_o, \bar{c}_o) = \frac{N}{S(D)} \sqrt{\frac{\delta\kappa^2(D)(K_0 - \boldsymbol{K}^T \boldsymbol{\mathcal{K}}^{-1} \boldsymbol{K})}{\pi}} \Bigg|_{D=3}. \tag{81}$$

Thus we minimize the following quantity with respect to the two parameters $\bar{V}_o$ and $\bar{c}_0$:

$$R^2 = \sum_{i=1}^{6} [\bar{E}_i^{(DMC)} - \bar{E}^{(DPT)}(N_i; \bar{V}_o, \bar{c}_o)]^2 + \sum_{N=\{3,10\}} \{ [\bar{r}_{peak}^{(DMC)}(N) - \bar{r}_{peak}^{(DPT)}(N; \bar{V}_o, \bar{c}_o)]^2 + [N_{max}^{(DMC)}(N) - (N_0)_{max}^{(DPT)}(N; \bar{V}_o, \bar{c}_o)]^2 \}, \tag{82}$$

where $\bar{E}_i^{(DMC)}$ is the dimensionally scaled DMC energy for a condensate with atom number N_i, while $\bar{r}_{peak}^{(DMC)}(N)$ and $N_{max}^{(DMC)}(N)$ are the dimensionally scaled position and height of the peak of the DMC density profile. The quantity $\bar{E}^{(DPT)}(N_i; \bar{V}_o, \bar{c}_o)$ is the DPT energy approximation through harmonic order given by Eqs. (25) with interatomic potential parameters $\bar{V}_o$ and $\bar{c}_o$, evaluated at $D=3$. Thus we have a two-parameter fit for $\bar{c}_o$ and $\bar{V}_o$. This results in values $c_o=0.9690$ and $V_o=0.0207$ at an R^2 of 0.5415.

We remind the reader that the potential at $D=3$ remains a simple hard-sphere potential at $r=a$.

XII. RESULTS AND DISCUSSION

In Fig. 1 we plot the Jacobian-weighted density profile divided by the number of atoms N at $N=100$ for a scattering

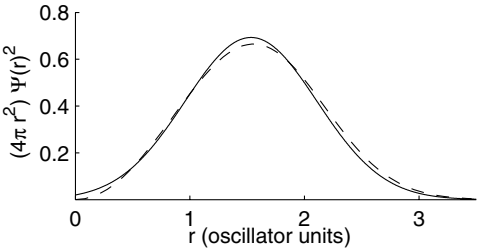

FIG. 1. The harmonic-order number density per atom vs radial distance of a spherically confined BEC of 100 ^{87}Rb atoms with $a=1000$ a.u. and $\omega_{ho}=2\pi\times 77.87$ Hz. The solid line is the analytic DPT density and the dashed line is the MGP density. Both curves are weighted by the Jacobian.

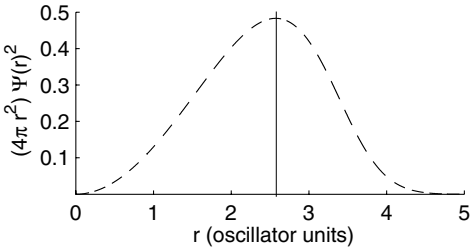

FIG. 2. The MGP number density per atom vs radial distance of a spherically confined BEC of 1000 ^{87}Rb atoms with $a=1000$ a.u. and $\omega_{ho}=2\pi\times 77.87$ Hz. The dashed line is the MGP density weighted by the Jacobian. The vertical line is inserted to emphasize the asymmetry of the MGP curve at higher N.

length $a/a_{ho}=0.0433$, or roughly ten times the natural scattering length of ^{87}Rb when $\omega_{ho}=2\pi\times 77.87$ Hz. One hundred atoms is a tenfold increase over the largest N density profile initially used to determine the interatomic potential parameters $\bar{c}_o$ and $\bar{V}_o$. As we see, the DPT density profile lies close to the MGP result, particularly in the $0.5\leqslant r/a_{ho}\leqslant 1$ range, although the peak of the DPT profile is a little higher. Since the area under the curve is normalized to 1, the extra height of the DPT peak comes at the expense of density at larger values of r/a_{ho} which lies below both the GP and MGP result. At larger values of N the density profile develops an asymmetric aspect. This is illustrated in Fig. 2 where we plot the MGP Jacobian-weighted density profile at the same scattering length for $N=1000$. The lowest-order DPT density profile of Eq. (68) is a Gaussian and symmetric about $r_{peak}^{(DPT)}(N;\bar{V}_o,\bar{c}_o)$, and so is unable to capture this emerging asymmetry as N increases. Also if we fix N and increase the scattering length yet further, the density profile becomes increasingly asymmetric. Thus while the harmonic-order DPT density profile is reasonably accurate for small a and for smaller N at intermediate a, incorporating beyond-mean-field effects for more strongly interacting systems (larger N or a) means we need to go to next order beyond harmonic in the DPT perturbation expansion to achieve an asymmetric beyond-mean-field Jacobian-weighted density profile.

A next-order calculation for more strongly interacting systems may be outlined as follows. The higher-order beyond-harmonic interaction terms have to be re-expressed in terms of the normal coordinates of the large-D system. In this regard the S_N symmetry greatly simplifies this task since the interaction terms individually have to transform under the scalar $[N]$ irreducible representation of S_N. In particular, there are only a finite number of Clebsch-Gordon coefficients of S_N coupling a finite number of normal coordinates, which transform under the three above discussed irreducible representations of S_N, together to form a scalar $[N]$ irrep. For example, there are only eight Clebsch-Gordon coefficients of S_N which couple three normal coordinates transforming under the $[N]$, $[N-1,1]$, or $[N-2,2]$ irreducible representations together to form a scalar $[N]$ irrep. Actually, it is this limited number of Clebsch-Gordon coefficients which has allowed for the essentially analytic solution discussed in this paper of the harmonic-order DPT approximation and it greatly simplifies the higher-order beyond-harmonic interaction terms and their necessary transformation to normal coordinates. The required Clebsch-Gordon coefficients may be calculated analytically for arbitrary N.

XIII. CONCLUSIONS

In this paper we have calculated an N-body, analytic, lowest-order DPT Jacobian-weighted density profile for a quantum confined system with a general two-body interaction from the previously derived analytic lowest-order DPT wave function [18]. The density profile is directly observable for macroscopic quantum confined systems, such as a BEC.

The theory applied in this paper for $L=0$ states of spherically confined systems is applicable to systems with attractive or repulsive interparticle interactions and is also applicable to both weakly (mean field) and strongly (beyond-mean-field) correlated systems. As we have noted above, the fact that $\bar{\gamma}_\infty$ is not zero is an indication that beyond-mean-field effects are included in this result even in the $D\to\infty$ limit. This theory is readily generalizable to systems for which the confining potential has cylindrical symmetry.

We have applied the general formalism for the harmonic-order DPT Jacobian-weighted density profile developed in this paper to the example of a spherically confined BEC. The higher-order DPT terms are minimized by analytically continuing the interatomic potential in D away from a hard sphere of radius a at $D=3$ so that we fit closely to accurate low-N DMC energies and Jacobian-weighted density profiles ($N=3$ and 10 for the density profiles). We have chosen a scattering length $a/a_{ho}=0.0433$, or roughly ten times the natural scattering length of ^{87}Rb when $\omega_{ho}=2\pi\times 77.87$ Hz. At this value of a the beyond-mean-field MGP equation remains valid for comparison. Exploiting the fact that our result is largely analytic, so that the particle number N is a parameter in our theory, we have tested the Jacobian-weighted density profile at $N=100$ and find the DPT result to lie close to the MGP result.

However, for more strongly interacting systems the Jacobian-weighted density profile develops an asymmetry about the peak that our harmonic-order DPT Jacobian-

weighted density profile does not mimic. Thus higher-order calculations are required for larger N and large a. A detailed program for calculating higher-order DPT corrections to N-body systems has been laid out in the paper by Dunn *et al.* [15] and has been applied to high order for small-N systems [34]. As discussed at the end of Sec. XII of this paper, for large-N systems the S_N point-group symmetry is at the heart of, and greatly simplifies, the calculation of these higher-order terms.

ACKNOWLEDGMENTS

We acknowledge continued support from the Army Research Office. We thank Doerte Blume for DMC results.

[1] See, for example, L. P. Kouwenhoven, D. G. Austing, and S. Tarucha, Rep. Prog. Phys. **64**, 701 (2001).
[2] See, for example, P. Benetatos and M. C. Manchetti, Phys. Rev. B **65**, 134517 (2002).
[3] See, for example, W. Ketterle, Rev. Mod. Phys. **74**, 1131 (2002); E. A. Cornell and C. E. Wieman, *ibid.* **74**, 875 (2002); A. J. Leggett, *ibid.* **73**, 307 (2001); L. Pitaevskii and S. Stringari, *Bose-Einstein Condensation* (Oxford University Press, Oxford, 2003).
[4] See, for example, K. B. Whaley, in *Advances in Molecular Vibrations and Collision Dynamics*, edited by J. Bowman (JAI Press, Greenwich, CN, 1998), Vol. 3; J. P. Toennies, A. F. Vilesov, and K. B. Whaley, Phys. Today **54**(2), 31 (2001).
[5] A. Minguzzi, S. Succi, F. Toschi, M. P. Tosi, and P. Vignolo, Phys. Rep. **395**, 223 (2004); J. O. Anderson, Rev. Mod. Phys. **76**, 599 (2004).
[6] See, for example, L. S. Cederbaum, O. E. Alon, and A. I. Streltsov, Phys. Rev. A **73**, 043609 (2006).
[7] See, for example, S. Fantoni and A. Fabrocini, in *Microscopic Quantum Many Body Theories and Their Applications*, Lecture Notes in Physics Vol. 150, edited by J. Navarro and A. Polls (Springer-Verlag, Berlin, 1998), p. 119; A. Fabrocini and A. Polls, Phys. Rev. A **60**, 2319 (1999).
[8] A. Banerjee and M. P. Singh, Phys. Rev. A **64**, 063604 (2001).
[9] See, for example, D. Landau and K. Binder, *A Guide to Monte-Carlo Simulations in Statistical Physics* (Cambridge University Press, Cambridge, England, 2001); M. Holzmann, W. Krauth, and M. Naraschewski, Phys. Rev. A **59**, 2956 (1999); J. K. Nilsen, J. Mur-Petit, M. Guilleumas, M. Hjorth-Jensen, and A. Polls, *ibid.* **71**, 053610 (2005); J. L. DuBois and H. R. Glyde, *ibid.* **63**, 023602 (2001).
[10] D. Blume and C. H. Greene, Phys. Rev. A **63**, 063601 (2001).
[11] *Dimensional Scaling in Chemical Physics*, edited by D. R. Herschbach, J. Avery, and O. Goscinski (Kluwer, Dordrecht, 1992).
[12] A. Chatterjee, Phys. Rep. **186**, 249 (1990).
[13] B. A. McKinney, M. Dunn, D. K. Watson, and J. G. Loeser, Ann. Phys. (N.Y.) **310**, 56 (2003).
[14] B. A. McKinney, M. Dunn, and D. K. Watson, Phys. Rev. A **69**, 053611 (2004).
[15] M. Dunn, T. C. Germann, D. Z. Goodson, C. A. Traynor, J. D. Morgan III, D. K. Watson, and D. R. Herschbach, J. Chem. Phys. **101**, 5987 (1994).
[16] W. B. Laing, M. Dunn, D. K. Watson, and J. G. Loeser, e-print physics/0510177.
[17] J. G. Loeser, J. Chem. Phys. **86**, 5635 (1987).
[18] M. Dunn, D. K. Watson, and J. G. Loeser, Ann. Phys. (N.Y.) **321**, 1939 (2006).
[19] E. B. Wilson, Jr., J. C. Decius, and P. C. Cross, *Molecular Vibrations: The Theory of Infrared and Raman Vibrational Spectra* (McGraw-Hill, New York, 1955).
[20] See, for example, M. Hamermesh, *Group Theory and Its Application to Physical Problems* (Addison-Wesley, Reading, MA, 1962).
[21] J. Avery, D. Z. Goodson, and D. R. Herschbach, Theor. Chim. Acta **81**, 1 (1991).
[22] Actually, in the case of CH_4 the carbon atom should be positioned away from the four hydrogens in a fourth dimension orthogonal to the three-dimensional subspace spanned by the hydrogen atoms. The position of the carbon in the actual $D=3$ methane molecule represents the point of intersection of this fourth dimension in which the carbon atom sits with the three-dimensional subspace spanned by the hydrogen atoms.
[23] S. T. Rittenhouse, M. J. Cavagnero, J. von Stecher, and C. H. Greene, e-print cond-mat/0510454.
[24] A. Chatterjee, J. Phys. A **18**, 735 (1985).
[25] See Z. Zhen and J. Loeser, in *Dimensional Scaling in Chemical Physics* (Ref. [11]), Chap. 3, p. 90.
[26] G. N. Lewis, J. Am. Chem. Soc. **38**, 762 (1916).
[27] I. Langmuir, J. Am. Chem. Soc. **41**, 868 (1919).
[28] G. Strang, *Linear Algebra and Its Applications*, 3rd ed. (Harcourt Brace Jovanovich College Publishers, Orlando, FL, 1988).
[29] M. Dunn, W. B. Laing, and D. K. Watson (unpublished).
[30] Since we are treating only $L=0$ states in a spherical trap in this paper, we do not address higher multipole excitations. Higher angular momentum states may be addressed using the formalism developed in M. Dunn and D. K. Watson, Ann. Phys. (N.Y.) **251**, 266 (1996); **251**, 319 (1996).
[31] See, for example, Ref. [19], Appendix XII, p. 347.
[32] J. Avery, *Hyperspherical Harmonics; Applications in Quantum Theory* (Kluwer Academic, Dordrecht, 1989).
[33] E. Braaten and A. Nieto, Phys. Rev. B **56**, 14745 (1997); E. Timmermans, P. Tommasini, and K. Huang, Phys. Rev. A **55**, 3645 (1997).
[34] J. R. Walkup, M. Dunn, D. K. Watson, and T. C. Germann, Phys. Rev. A **58**, 4668 (1998); J. C. Carzoli, M. Dunn, and D. K. Watson, *ibid.* **59**, 182 (1999); J. R. Walkup, M. Dunn, and D. K. Watson, J. Math. Phys. **41**, 218 (2000); Phys. Rev. A **63**, 025405 (2000).